

Chaos in a periodically forced chemostat with algal mortality

Sébastien Clodong and Bernd Blasius*

Department of Physics, University of Potsdam, Am Neuen Palais 10, D-14415 Potsdam, Germany

We study the possibility of chaotic dynamics in the externally driven Droop model. This model describes a phytoplankton population in a chemostat under periodic nutrient supply. Previously, it has been proven under very general assumptions, that such systems are not able to exhibit chaotic dynamics. We show that the simple introduction of algal mortality may lead to chaotic oscillations of algal density in the forced chemostat. Our numerical simulations show that the existence of chaos is intimately related to plankton overshooting in the unforced model. We provide a simple measure, based on stability analysis, for estimating the amount of overshooting. These findings are not restricted to the Droop model but also hold for other chemostat models with mortality. Our results suggest periodically driven chemostats as a simple model system for the experimental verification of chaos in ecology.

Keywords: Droop model; chaos; chemostats; periodically forced system; nutrient-limited algal growth; algal mortality

1. INTRODUCTION

Ever since Robert May's discovery of irregular behaviour in the simple logistic equation (May 1974), ecologists have been fascinated by the possibility that similar chaotic dynamics may be exhibited by natural systems, and thus could be responsible for the commonly observed fluctuations in population numbers (Hastings *et al.* 1993; Blasius *et al.* 1999; Cushing *et al.* 2003). Besides the logistic equation, many or most ecological models allow for chaotic solutions because of several generic mechanisms such as nonlinear internal regulations, time delayed feedback or periodic external forcing (Hastings & Powell 1991; Costantino *et al.* 1997; Blasius *et al.* 1999; Blasius & Stone 2000). Despite this ubiquity of chaotic regimes in the standard ecological models, there are few examples where the theoretical concepts could successfully be translated into real case studies and hard data (see Cushing *et al.* 2003). These difficulties arise, to some extent, from the common shortage of ecological time-series. However, other problems are inherent in the systems themselves, which can never be isolated from their environment and therefore necessarily are subject to major disturbances and noise (Dennis *et al.* 2003).

One promising approach to deal with such problems is to bring nature into the laboratory. Recently, the method of continuous chemostats, as an experimental system for the growth of micro-organisms such as phytoplankton, has been proven to be a powerful experimental set-up that allows a successful combination of theoretical concepts with ecological reality (Smith & Waltman 1995; Fussmann *et al.* 2000; Yoshida *et al.* 2003). Most studies of chemostat dynamics have focused on ideal constant-nutrient environments. In recent years, however, there has been renewed interest in the nutrient-limited growth of phytoplankton in environments with variable nutrient levels. For example, it has been found that time-variable

conditions may promote the coexistence of competing phytoplankton species (Hutchinson 1961; Sommer 1985; Ebenhöh 1988; Huisman & Weissing 1999).

Non-equilibrium conditions are ubiquitous in ecology. Almost without exception biological communities are affected by perturbations that frequently show more or less periodic patterns. Consequently, the effects of periodic forcing on ecological models (Kot *et al.* 1992; Rinaldi & Muratori 1993; Earn *et al.* 2000; Vandermeer *et al.* 2001) and on phytoplankton models (Ebenhöh 1988, 1993; Truscott 1995) have been intensively studied. All these studies confirm that, typically, periodic forcing can drive the biological system into a chaotic regime if the strength of forcing is sufficiently large. Astonishingly, however, externally driven chemostats of a single species seem to be an exception to this general rule. In such systems common wisdom forbids the appearance of chaotic solutions because of external forcing (Pascual 1994; Smith 1997).

The classical model for describing the nutrient-limited growth of phytoplankton in a chemostat dates back to Monod (1942). This simple model is able to capture the basic characteristics of the algal dynamics but has been criticized because it relates the growth of phytoplankton directly to the nutrient uptake. These model assumptions are refined in the Droop model, which essentially decouples algal growth from nutrient uptake (Droop 1968, 1973) and can now be regarded as the paradigmatic model to describe the growth of phytoplankton in a chemostat (DeAngelis 1992; Lange & Oyarzun 1992).

It has long been known that chaotic dynamics are not possible in the periodically driven Monod model. More complex behaviour was expected to arise in the Droop model because the passage of nutrients from the outside to the inside of the cell introduces inevitable time-delays. It was argued that such delays might play an important role in non-equilibrium situations (Lange & Oyarzun 1992; Pascual 1994). The consequences of periodic influence on the Droop model were first studied by Pascual (1994), where it was found that chaotic dynamics did not

* Author for correspondence (bernd@agnld.uni-potsdam.de).

occur. Later, these studies were extended to various generalizations of the Droop model; however, always with the same negative result. In all the investigated model variations the existence of chaos could rigorously be excluded (Smith 1997). These results led to the belief that externally forced chemostats of a single species are unable to exhibit chaotic dynamics, in this way ruling out such systems as a candidate for the experimental verification of chaos.

We explore this case in more detail, and show that simple chemostats can give rise to greater complexity than was previously thought. As we demonstrate, the simple introduction of an additional algal loss or mortality allows for the existence of chaotic solutions. Algal mortality usually plays only a minor role in the laboratory system because the residence time of the cells in the chemostat is much smaller than their average lifespan. Therefore, algal mortality is usually neglected in chemostat models. Nevertheless, it is also possible to realize an effective algal mortality in the experimental situation, for example in the form of an auxiliary flow-loop in which phytoplankton is filtered out of the water column (G. Fussmann, personal communication). As we demonstrate, this innocent modification of the system has fundamental dynamical consequences and, for example, allows for the appearance of chaos.

2. THE MODEL

The Droop model (Droop 1968, 1973) has been well studied in the past decade (see Lange & Oyarzun (1992) for a detailed analysis). The model describes a well-stirred reactor that contains phytoplankton cells with concentration $P(t)$ in a growth medium of limiting nutrients with concentration $N(t)$. Each phytoplankton cell is assumed to possess an internal pool of stored nutrients (the so-called cell quota) $Q(t)$. The chemostat is supplied with nutrients at input concentration $N_i(t)$ from an external nutritive medium. Note that we allow the external nutrient supply to be a function of time, t . The outflow contains both medium and phytoplankton cells. Inflow and outflow are characterized by the dilution rate D . Under these assumptions the Droop model takes the following form:

$$\begin{aligned} \dot{N} &= D(N_i(t) - N) - \rho(N)P, \\ \dot{P} &= \mu(Q)P - (M + D)P, \\ \dot{Q} &= \rho(N) - \mu(Q)Q, \end{aligned} \tag{2.1}$$

with

$$\mu(Q) = \mu_m \left(1 - \frac{K_Q}{Q} \right) \text{ and } \rho(N) = \rho_m \frac{N}{K_p + N}. \tag{2.2}$$

It is assumed that the phytoplankton growth rate $\mu(Q)$ depends solely on the cell quota. μ_m is the maximal growth rate and K_Q is the minimal amount of nutrients per phytoplankton cell, i.e. $Q(t) > K_Q$. $\rho(N)$ represents the nutrient assimilation rate of the phytoplankton cells and is modelled as a Monod function with maximum uptake rate ρ_m and half saturation constant K_p . Furthermore, we modify the model by the introduction of an additional phytoplankton mortality M .

For further analysis, we rewrite the model (2.1) in non-dimensional variables:

$$\begin{aligned} \dot{n} &= \delta(n_i(\tau) - n) - \frac{np}{1+n}, \\ \dot{p} &= \left(1 - \frac{1}{q} \right) p - (m + \delta)p, \\ \dot{q} &= \frac{\alpha n}{1+n} + 1 - q. \end{aligned} \tag{2.3}$$

Here, the variable transformations

$$n = \frac{N}{K_p}, \quad p = \left(\frac{\rho_m}{\mu_m K_p} \right) P, \quad q = \frac{Q}{K_q}, \quad \tau = \mu_m t \tag{2.4}$$

have been performed and the new parameters are

$$m = \frac{M}{\mu_m}, \quad \delta = \frac{D}{\mu_m}, \quad n_i = \frac{N_i}{K_p}, \quad \alpha = \frac{\rho_m}{\mu_m K_q}. \tag{2.5}$$

In dimensionless units the model contains only four independent control parameters: the effective phytoplankton mortality m , the dilution rate δ and the input nutrient concentration n_i , all of which can be controlled in the experiment, and the parameter α , which is related to the physiology of the phytoplankton species. Note that the dimensionless variables are restricted to the range $n, p \geq 0, q \geq 1$. Besides the Droop model (equation (2.3)) we also study the more simplistic Monod model (equation (A 3)), which arises in the limit $\alpha \ll 1$, i.e. when the algal growth rate is small in comparison to the uptake rate (see Appendix A).

3. STABILITY ANALYSIS OF THE UNFORCED MODEL

Following Lange & Oyarzun (1992) we first analyse the stability of system (2.3) without any external forcing, i.e. when the supply of input nutrients is constant $n_i(t) = n_i$. The system then contains two fixed points. The first fixed point describes a steady state without phytoplankton and is given by

$$(n_1^*, p_1^*, q_1^*) = \left(n_i, 0, 1 + \frac{\alpha n_i}{1+n_i} \right). \tag{3.1}$$

By contrast, the second fixed point

$$(n_2^*, p_2^*, q_2^*) = \left(\frac{d}{\alpha(1-d) - d}, \delta(n_i - n_2^*) \frac{\alpha(1-d)}{d}, \frac{1}{1-d} \right) \tag{3.2}$$

represents a non-vanishing algal concentration. Here, $d = m + \delta$ represents the total phytoplankton loss rate, which acts as a main bifurcation parameter. Note that p_2^* depends linearly on the difference between input nutrients n_i and nutrient equilibrium n_2^* . Both fixed points collide at the critical value

$$d_c = \frac{\alpha n_i}{1 + (1 + \alpha)n_i}. \tag{3.3}$$

In the case of large loss rate, $m + \delta > d_c$, the trivial equilibrium (equation (3.1)) is stable and the algae are washed out of the chemostat. In this regime, equation (3.1) has the stability type of a stable star, i.e. all three eigenvalues of the Jacobian are negative $(-, -, -)$. By contrast, if the total loss rate is smaller than the threshold, $m + \delta < d_c$, the equilibrium (3.1) is unstable whereas equation (3.2) becomes

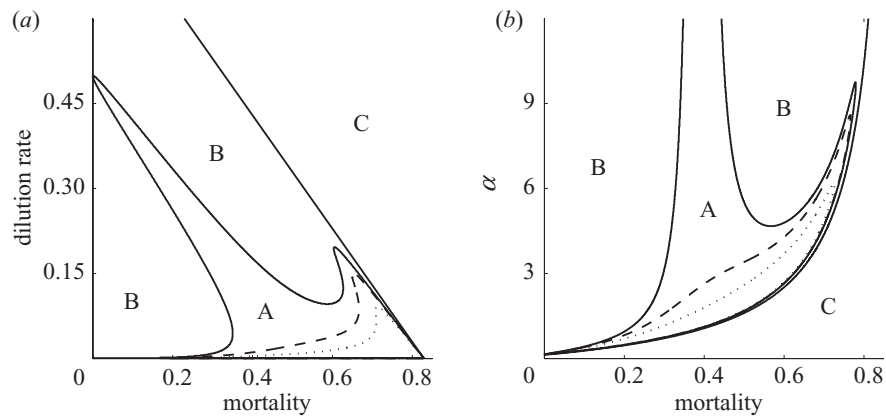


Figure 1. (a) Stability diagram of the unforced Droop model (equation (2.3)) showing the regimes in parameter space with a stable spiral (A), a stable node (B) and algal washout (C). (a) Results in (m, δ) parameter plane for $\alpha = 5$, $n_i = 40$ and (b) results in (m, α) plane for $\delta = 0.11$, $n_i = 40$. Also shown is the estimate of plankton overshooting κ in the spiral regime calculated by equation (3.5). Lines are plotted where the overshooting measure takes the constant values $\kappa = \kappa_1$ (dotted line) and $\kappa = \kappa_2$ (dashed line). Parameters: (a) $\kappa_1 = 10^{-2}$ and $\kappa_2 = 10^{-4}$; (b) $\kappa_1 = 10^{-3}$ and $\kappa_2 = 10^{-6}$.

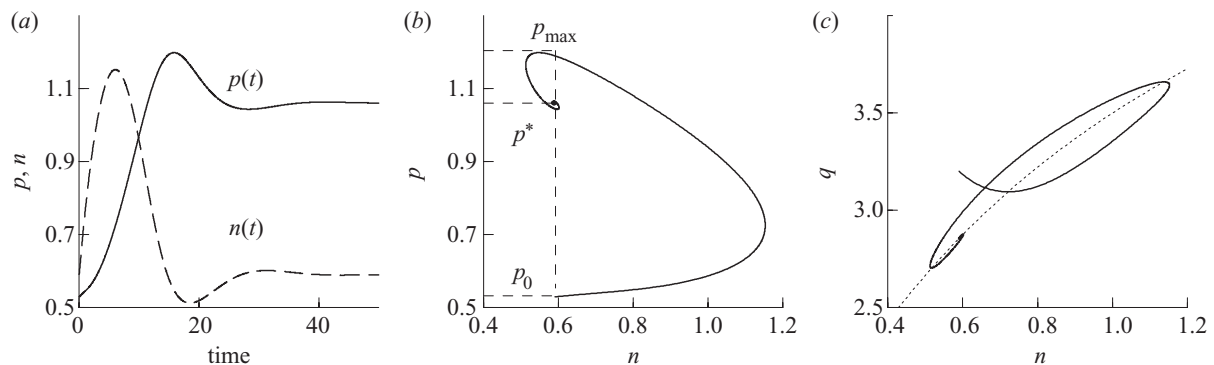


Figure 2. Typical behaviour of the unforced model (equation (2.3)) in the spiral regime. (a) The time-series of phytoplankton $p(\tau)$ and nutrients $n(\tau)$; (b,c) the resulting trajectories in the (n, p) - and (n, q) -planes, respectively. In (c) the functional dependence $q(n)$ (equation (A 2)) is also drawn (dotted line). Also shown in (b) is a schematic representation of p^* , p_{\max} and p_0 . Parameter values $m = 0.64$, $\delta = 0.01$, $n_i = 40$, $\alpha = 5$, and initial values $n_0 = n^* = 0.59$, $p_0 = p^*/2 = 0.53$, $q_0 = 3.2$. The eigenvalues of the stable spiral are $\lambda_1 = -1.12$, $\lambda_{2,3} = -0.153 \pm 0.25i$.

positive and stable. Thus, at $d = d_c$ both fixed points exchange their stability in a transcritical bifurcation. Stable coexistence of nutrients and phytoplankton is possible only for $d < d_c$. Depending on the parameter set, equation (3.2) may then either have the stability type of a stable star $(-, -, -)$ or of a stable spiral $(-, +i, -i)$. Figure 1 presents a visualization of these different regimes in the parameter planes (m, δ) and (m, α) . Very similar stability properties arise in the Monod model (equation (A 3)). In particular, depending on the parameter set there are also two different steady-state solutions of either algal washout or stable phytoplankton–nutrient coexistence. In the Monod model equation (3.3) must be replaced by $d'_c = n_i/(1 + n_i)$.

Notice from the stability diagram in figure 1 that spiral solutions are only allowed with explicit algal mortality, i.e. if $m > 0$. Therefore, one noticeable effect of phytoplankton mortality is the ability to modify the topology of the non-trivial fixed point from a stable star to a stable spiral, in this way allowing the phytoplankton to undergo damped oscillations before reaching equilibrium. As will be shown, this difference has important consequences under external forcing.

Figure 2 depicts a typical simulation result with $m > 0$ in the region with a stable spiral. Clearly phytoplankton

does not reach equilibrium monotonically but goes through an intermediate maximum value. This overshooting of phytoplankton is a direct consequence of the spiral geometry in the (n, p) -phase plane (see figure 2b). As shown in figure 2c the cell quote q closely follows the nutrient concentration (see also Appendix A), and in three-dimensional-phase space the trajectory forms a flat spiral. This geometry is also reflected in the eigenvalue spectrum of the stable equilibrium (equation (3.2)). The eigenvalue corresponding to the eigenvector \mathbf{v}_1^+ , which is directing out of the plane of the spiral, is a negative number, $\lambda_1 < 0$. By contrast, the other two eigenvectors \mathbf{v}_2^+ and \mathbf{v}_3^+ are located in the plane of the spiral and the corresponding eigenvalues form a pair of complex conjugate numbers with negative real part, $\lambda_{2,3} = -\rho \pm i\omega$; the eigenvalue is decomposed into its real and imaginary parts. Our numerical investigations show that the absolute value of λ_1 is approximately one order of magnitude larger than that of the other two eigenvalues, $\lambda_1 \ll -\rho$ (see legend to figure 2). Therefore, any perturbation of the system out of the plane of the spiral is very quickly re-attracted.

We now introduce a quantity that allows measurement of the strength of phytoplankton overshooting. Obviously the imaginary part ω of the eigenvalues alone is not

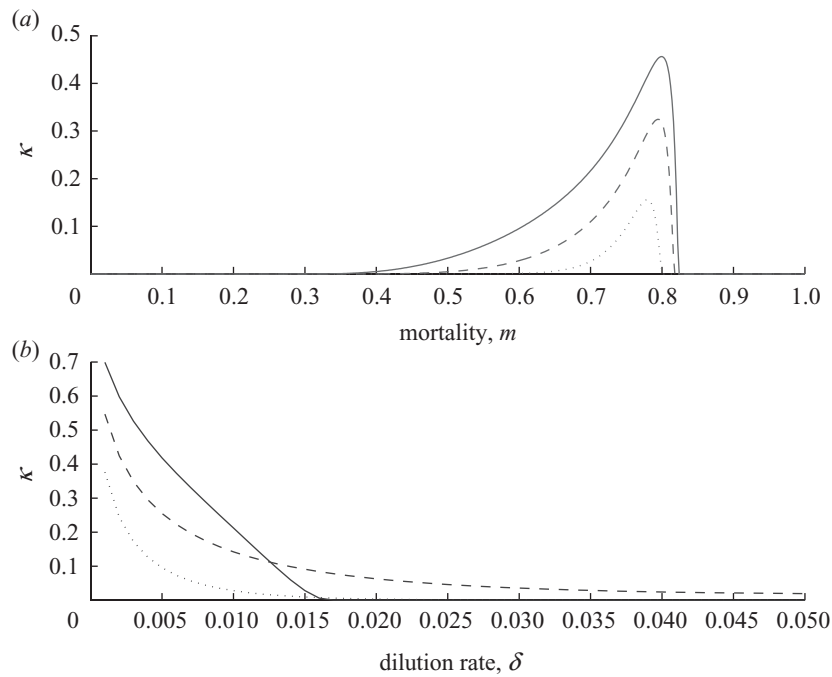


Figure 3. Overshooting as a function of mortality m and dilution rate δ , showing the measure of plankton overshooting κ calculated by equation (3.5). (a) κ as a function of m for $\delta = 0.005$ (solid line), $\delta = 0.01$ (dashed line), $\delta = 0.025$ (dotted line). (b) κ as a function of δ for $m = 0.81$ (solid line), $m = 0.72$ (dashed line) and $m = 0.60$ (dotted line).

sufficient because it contains only information about the rotation speed of the spiral but not about the damping. In fact, we observe that the ratio ρ/ω of real and imaginary parts gives a good characterization. This becomes clear by inspection of figure 2*b*. Starting from initial conditions (n^*, p_0) which in phase space are located with a vertical distance $p^* - p_0$ exactly below the fixed point, we estimate the height of the following intermediate phytoplankton maximum, p_{\max} . The ratio $\kappa = (p_{\max} - p^*) / (p^* - p_0)$ is then a measure for the damping of the oscillation amplitude over half a cycle. In the neighbourhood of the fixed point we can use the linearization of the model around the fixed point to calculate κ . Assuming first a two-dimensional spiral simple algebra leads to the formula

$$\kappa = \frac{p_{\max} - p^*}{p^* - p_0} = e^{-\pi\rho/\omega}, \tag{3.4}$$

where $\rho = -\text{Re}(\lambda_i)$ is the damping rate and $\omega = |\text{Im}(\lambda_i)|$ is the typical rotation frequency around the fixed point. Note, that κ in equation (3.4) is independent of the initial point ρ_0 .

Equation (3.4) holds for the two-variable Monod model. The corresponding results for the full Droop model are slightly more involved. Solving the eigenvalue and eigenvector problem for the Jacobian matrix in the Droop model (equation (2.1)) and assuming a flat spiral in phase space, i.e. $n_0 \approx n(\pi/\omega) \approx n^*$ and $q_0 \approx q(\pi/\omega) \approx q^*$, leads to the formula

$$\frac{p_{\max} - p^*}{p^* - p_0} = \frac{1}{\varepsilon} \left[\left(\frac{\lambda_2 - \lambda_3}{\lambda_1} \right) e^{\pi\lambda_1/\omega} - \left(\frac{\lambda_3 - \lambda_1}{\lambda_2} \right) e^{\pi\text{Re}(\lambda_{2,3})/\omega} - \left(\frac{\lambda_1 - \lambda_2}{\lambda_3} \right) e^{\pi\text{Re}(\lambda_{2,3})/\omega} \right], \tag{3.5}$$

where ω is the absolute value of the two non-zero $\text{Im}(\lambda_i)$ and

$$\varepsilon = (\lambda_2 - \lambda_3)/\lambda_1 + (\lambda_3 - \lambda_1)/\lambda_2 + (\lambda_1 - \lambda_2)/\lambda_3.$$

In figures 1 and 3, numerically obtained values for the plankton overshooting, κ , in the unforced Droop model (equation (2.3)) are plotted in dependence on various control parameters. In general, maximal overshooting takes place for large algal mortality and comparatively small dilution rates. We want to stress that the overshooting measure κ is not restricted to chemostat models but holds as well for other systems with spiral dynamics, and therefore is applicable under quite general circumstances. In many practical situations the quantities of main interest are not only the equilibria of the system, but also the maximal abundance that can be attained by the system on its transition towards equilibrium. In such cases our simple formula (equation (3.4)) provides a comfortable method for the estimation of the amount of overshooting.

4. CHAOTIC DYNAMICS WITH PERIODIC FORCING

We now introduce external forcing into the model (equation (2.3)) by taking the input nutrient concentration $n_i(\tau)$ to be a periodic function of time. For simplicity, we choose a square wave forcing where the external medium contains nutrients of concentration n_i^{\max} during half of the forcing period T and is nutrient free the remainder of the time

$$n_i(\tau) = \begin{cases} n_i^{\max} & \text{for } kT \leq \tau < \left(k + \frac{1}{2}\right)T \quad (k = 0, 1, 2, \dots) \\ 0 & \text{otherwise.} \end{cases} \tag{4.1}$$

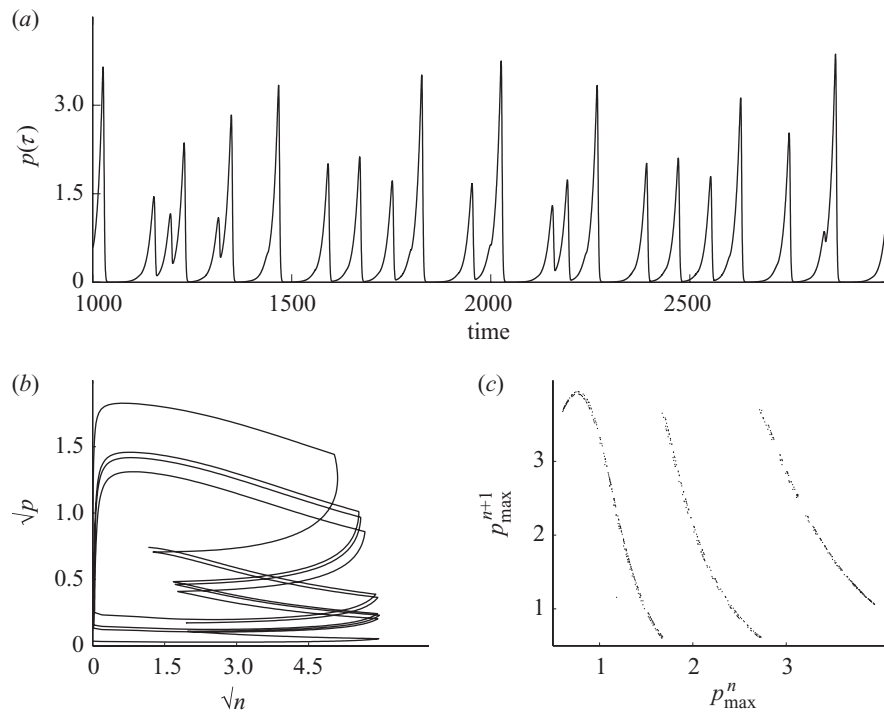


Figure 4. Typical simulation result of the forced system in the chaotic regime. (a) Time-series of phytoplankton $p(\tau)$; (b) chaotic attractor in the (n, p) phase plane (square-root-transformed variables); and (c) return map of successive phytoplankton maxima p_{\max} . Parameter values are $T = 40$, $\delta = 0.11$, $m = 0.64$, $\alpha = 5$ and $n_i^{\max} = 40$.

In our numerical simulations the periodic driving in general leads to forced oscillations of the algal abundance. However, in the presence of algal mortality large parameter regimes with chaotic solutions are also observed. A typical phytoplankton time-series in the chaotic regime is shown in figure 4a. Algal abundance undergoes recurrent out-breaks of irregular amplitude and timing. Figure 4b depicts the chaotic attractor. For better visualization the square-root-transformed variables are plotted. Successive maxima of the phytoplankton levels p_{\max}^n follow an almost one-dimensional return map (see figure 4c). In the parameter range of figure 4 the return map is piecewise continuous and built up from three branches, which correspond to the solutions with one, two or three periods of forcing between two successive phytoplankton maxima. Note that the existence of a simple unique return map allows for a prediction of the height of future phytoplankton maxima.

Figure 4b reveals the mechanism of the chaotic dynamics. A typical ‘cycle’ starts with initially small numbers of phytoplankton and nutrients, i.e. in the lower left part of the (n, p) -phase plane. As soon as $n_i(\tau)$ is in the ‘high’ state, nutrients are linearly accumulated through external inflow. Because the input nutrient concentration is relatively large, $n_i^{\max} \gg 1$ (see later discussion), the nutrient assimilation rate is soon saturated and the quota settles to the asymptotic value $q(t) \approx \alpha + 1$. At this stage the cells are sufficiently filled with nutrients and the reserves are used for cell divisions. Consequently, phytoplankton numbers slowly start to build up exponentially, $p = \exp \gamma t$, with a growth constant $\gamma = \alpha/(1 + \alpha) - (m + \delta)$. This phase of exponential growth is clearly visible in the time-series of figure 4a and can also be verified by plotting phytoplankton numbers on a logarithmic scale. Multiplication of algal numbers continues until a certain threshold level is reached. This may take several cycles of nutrient forcing,

since the amount of nutrients that are accumulated in one period is limited. As a result, the state of the system moves upward in phase space in a characteristic zigzag trajectory (figure 4b). With increasing phytoplankton numbers the nutrient consumption also rises. In this critical stage, as soon as the external nutrient supply, $n_i(\tau)$, switches to zero the nutrient reserves are used up very fast. Having consumed all its resources, the algal population declines rapidly and the trajectory in phase space spirals down into the left lower corner. The decline continues until the next nutrient pulse arrives. At this instant, nutrient levels start to rise again and the next cycle begins. The time that is needed by the phytoplankton population to reach threshold depends sensibly on the initial phytoplankton levels and therefore also on the last maximal levels p_{\max} . This memory effect is responsible for the chaotic dynamics and gives rise to the simple return map of p_{\max} (see figure 4c).

Figure 5 shows the bifurcation diagram obtained by varying the forcing period T . For small forcing periods the phytoplankton shows limit-cycle oscillations. When T rises above a critical value a transition to the chaotic regime is initiated. In general, by increasing the forcing period the amplitude of oscillations is reduced and the average number of forcing cycles between two successive phytoplankton maxima increases. Finally, for very large forcing periods the chaotic regime is again destroyed. In figure 5 the largest Lyapunov exponent, λ , is also plotted. The positive value of λ for a large parameter range confirms that the irregular behaviour of the algal numbers is indeed chaos. The parameter range with chaotic behaviour is intersected by periodic windows. Note the exact correspondence of the regimes with positive Lyapunov exponent and irregular behaviour in the bifurcation diagram.

To investigate the size of the chaotic regions, in figure 6 we represent the largest Lyapunov exponent as a

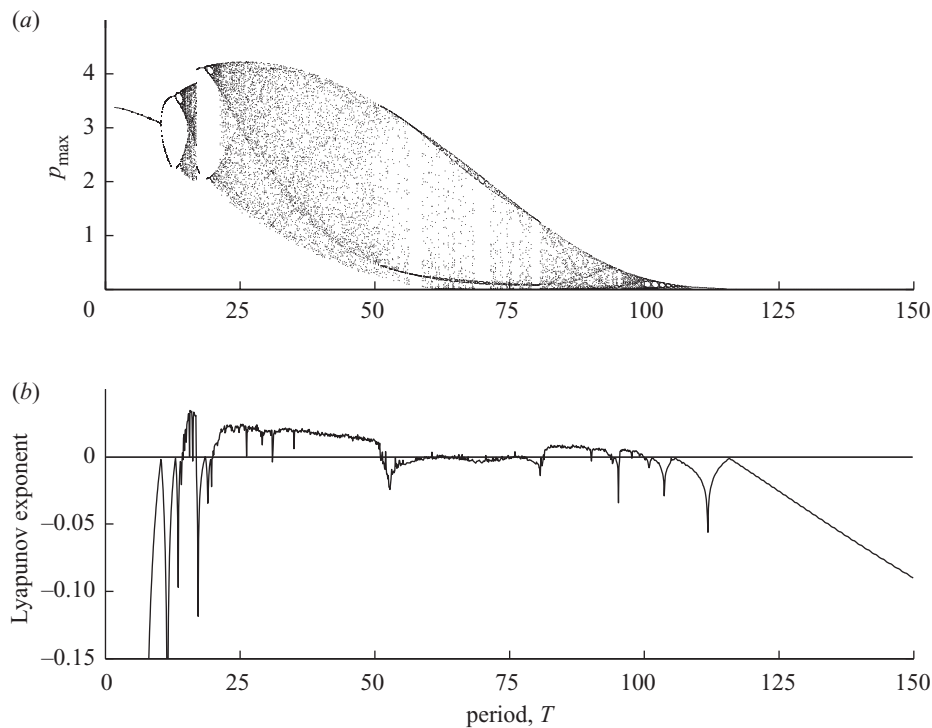


Figure 5. Bifurcation diagram. (a) The maxima of phytoplankton, p_{\max} and (b) the largest Lyapunov exponent computed with the Wolf algorithm (Wolf *et al.* 1985), dependent upon the forcing period T . Other parameters as in figure 4.

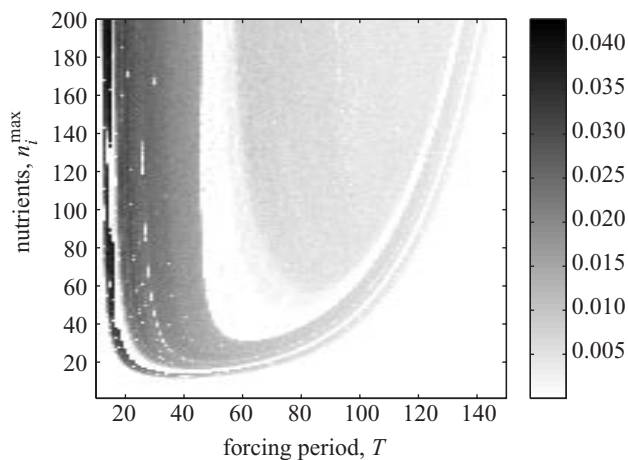


Figure 6. Largest Lyapunov exponent indicated as grey level in the (T, n_i^{\max}) parameter plane for the Droop model (equation (2.3)). Other parameters as in figure 4.

function of the two main forcing parameters, namely period of forcing T and forcing strength n_i^{\max} . In general, chaotic behaviour is found for a large range of forcing periods when n_i^{\max} is sufficiently large. In comparison, in figure 7 the largest Lyapunov exponent is plotted in the (m, δ) -parameter plane. Again, we find a broad regime with chaotic solutions. Very similar chaotic behaviour can be found in the forced Monod model (equation (A 3)) (see figure 7b). Interestingly, in both models the chaotic domain corresponds very well to the parameter values which lead to a large overshooting, i.e., a large value of κ , in the unforced model (compare also with figure 1). This observation indicates that the occurrence of spiral solutions in the unforced model is strongly related to the possibility of chaotic dynamics under external driving.

Owing to the introduction of algal mortality, the system undergoes damped oscillations, which interact with the external driving and generate complex dynamics.

One important question concerns the realism of the parameter values with chaotic behaviour of real experiments. As previously mentioned, the most crucial requirement for chaotic dynamics is the introduction of an additional algal mortality $m > 0$. Besides, we have been able to observe chaotic dynamics only when the concentration of input nutrients is rather large, $n_i^{\max} \gg 1$ (see figure 6). This condition ensures that nutrient assimilation is saturated during the phase of exponential algal growth as explained earlier. Note that the specific ‘square-wave’ forcing, which has been used, can easily be realized in the experiment. We have also investigated different forcing types, which in general lead to very similar results. However, it seems to be crucial that the lower level of input nutrients is set very close to zero. The chaotic regime is also robust towards modifications of the other parameters α and δ . In general, relatively small values of dilution rate δ are required for chaos. Further, we have observed chaotic dynamics in the full physiological range of $\alpha = 0.1 \dots 50$. In the limiting case when α is very small, the Droop model changes into the Monod model with rescaled parameters (see Appendix A and figure 7).

To summarize, the parameter range with chaotic dynamics is very broad and no parameter fine-tuning is necessary to observe chaos. In our numerical simulations we have used parameter values that can easily be realized in chemostat experiments. For example, typical values of control parameters in dimensional units (Droop 1968; Grover 1991a,b) such as $N_i^{\max} = 400 \mu\text{mol l}^{-1}$, $D = 0.3 \text{ d}^{-1}$, $\mu_m = 2 \text{ d}^{-1}$, $\rho_m = 0.03 \mu\text{mol d}^{-1} \text{ cell}^{-1}$, $K_p = 30 \mu\text{mol l}^{-1}$, $K_Q = 0.003 \mu\text{mol cell}^{-1}$, $M = 1.2 \text{ d}^{-1}$ correspond to non-dimensional parameters of $\delta = 0.15$,

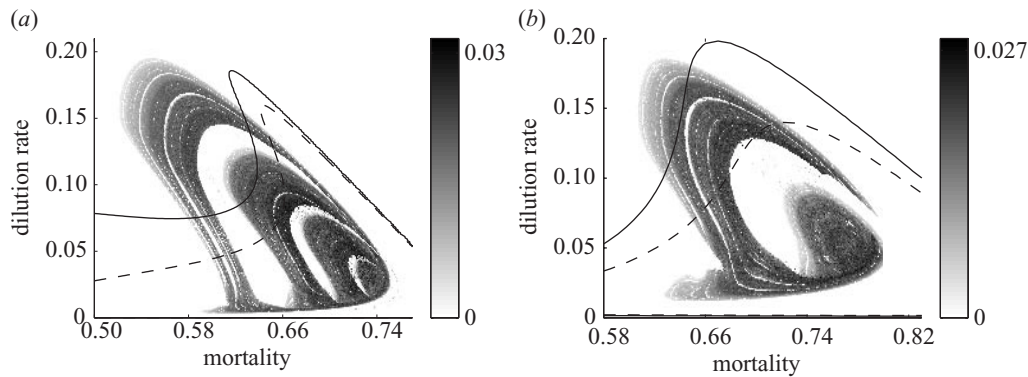


Figure 7. Largest Lyapunov exponent indicated as grey level in the (m, δ) parameter plane, for (a) the Droop model (equation (2.3)) with $T = 40$, and (b) the Monod model (equation (A 3)) with $T = 25$. Other parameters as in figure 4. Also shown are lines with constant value of overshooting κ of the unforced model: (a) solid line, $\kappa = 10^{-6}$, dashed line, $\kappa = 10^{-3}$; (b) solid line ($\kappa = 0.18$) and dashed line ($\kappa = 0.25$).

$m = 0.6$, $n_i^{\max} = 40$, $\alpha = 5$. In particular, we want to stress that the crucial condition of large input nutrient concentrations, $n_i^{\max} > 20$, is easily matched in real experiments.

Another experimental obstacle arises from the possibility of phytoplankton extinction events. In particular, if many external forcing cycles are needed during a typical chaotic cycle, in our numerical simulations phytoplankton numbers undergo changes of several orders of magnitude. In a chemostat with limited size this leads to the danger that phytoplankton may go extinct. However, in typical parameter ranges algal changes are in the range of four or five orders of magnitude, which is easily sustained in a chemostat, which may contain algal densities of up to 10^7 – 10^8 l^{-1} .

We have also investigated the robustness of our results. For example, we have checked other physiologically realistic monotonic growth functions as well as other forcing types, e.g. sinusoidal forcing. Typically, we found that the behaviour of the system is not greatly affected. In all these modifications of the model we have been able to observe large parameter regions with chaotic solutions when additional algal mortality was present. Furthermore, our results are robust under the influence of additive and multiplicative noise. For example, we have studied the system by replacing the growth rate or the uptake rate by a normally distributed random variable. In general, the inclusion of noise tends to enlarge only the domains with irregular fluctuations in the peak amplitudes. Note, however, that the notion of chaos, which originally is defined only for purely deterministic systems, is problematic in such noisy systems (see Dennis *et al.* 2003).

5. END DISCUSSION

We studied the dynamics of the periodically forced Droop model with an additional algal mortality. Recent chemostat studies have mostly focused on experiments with more than one species, either as competition studies or in predator–prey, i.e. nutrient–phytoplankton–zooplankton, cultures (Huisman & Weissing 1999; Fussmann *et al.* 2000; Yoshida *et al.* 2003). However, owing to the complexity of such systems these experiments are often difficult to perform and the measured time-series is not easy to interpret. By contrast, single-species chemostats are usually thought to give rise to only very poor dynamics.

For example, it has been proven that for $m = 0$ the Droop model cannot exhibit chaotic dynamics (Pascual 1994; Smith 1997). We have shown that even simple nutrient–phytoplankton cultures are able to exhibit complex behaviour. With the introduction of mortality the eigenvalues of the Jacobian matrix of the unforced system can become complex numbers, which allows the system to undergo damped oscillations before reaching equilibrium. Chaotic dynamics results upon the interaction of these damped oscillations with the time-periodic environment.

As mentioned in § 1, in the context of a continuous chemostat, algal mortality may be somewhat artificial, and in the laboratory experiment, must be realized by addition of an auxiliary circuit that filtrates part of the algae. In real aquatic ecosystems, however, the loss of algae from the epilimnion is of great relevance and arises mainly as a result of grazing by zooplankton and sinking into the deeper water layers. For example, it is well known that sinking algae act as a carbon pump and have a major impact on the global CO_2 cycle and climate regulation. Also, external nutrient forcing becomes a realistic feature owing to seasonal nutrient inflow and upwelling. In this sense the chaotic outbreaks of phytoplankton numbers in the forced chemostat model may have some significance for real aquatic ecosystems, where they would represent recurrent algal blooms. Similar results have been found in other simple models of bottom-up controlled phytoplankton systems (O’Brien 1974; Ebenhöf 1988; Huppert *et al.* 2002). Furthermore, taking all these effects into account, externally forced chemostats with additional mortality represent a simple yet realistic and controllable idealization of an aquatic system. In this respect our results are important for the design of new experiments.

Our results give an insight into the dynamics of nutrient-limited growth in a time-varying environment and contribute to the significance of chaos in ecology. We suggest a simple model system, which, in principle, allows experimental testing for chaos, and thus should be of relevance for the understanding and role of deterministic chaos in ecological systems.

This work was supported by German Volkswagen Stiftung. The authors thank G. Fussmann, A. Huppert and G. Weithaupt for discussions.

APPENDIX A: TRANSITION TO THE MONOD MODEL

In some limiting biological cases adiabatic elimination techniques can be applied to reduce the Droop model (equation (2.3)) to the more simplistic Monod model. We begin with the analytical solution for $q(\tau)$:

$$q(\tau) = 1 + \frac{\alpha n(\tau)}{1 + n(\tau)} + \left[q(\tau_0) - 1 - \frac{\alpha n(\tau_0)}{1 + n(\tau_0)} \right] e^{-(\tau - \tau_0)} - \alpha e^{-\tau} \int_{\tau_0}^{\tau} e^{\tau} \frac{\dot{n}(\tau)}{(1 + n(\tau))^2} d\tau. \quad (\text{A } 1)$$

If the parameter α is very small, $\alpha \ll 1$, it can be shown that the final two terms vanish after a time $\tau \gg 1$. The assumption $\alpha = \rho_m(\mu_m K_Q)^{-1} \ll 1$ corresponds to the limiting case where the maximal uptake rate μ_m is much larger than the maximal growth rate ρ_m . This means that after a time-scale $t \gg \mu_m^{-1}$, which corresponds to the typical time needed for cell division, the quotas are related to the nutrients with the functional dependence

$$q(\tau) \approx 1 + \frac{\alpha n(\tau)}{1 + n(\tau)}. \quad (\text{A } 2)$$

Inserting equation (A 2) into the second part of equation (2.3) and making the approximation $\alpha \ll 1$ leads to Monod's equations

$$\begin{aligned} \dot{s} &= \frac{ds}{d\tau'} = \delta'(n_i - s) - \frac{sx}{1 + s}, \\ \dot{x} &= \frac{dx}{d\tau'} = \frac{sx}{1 + s} - (m' + \delta')x \end{aligned} \quad (\text{A } 3)$$

with the following rescaled variables

$$s = n, x = \frac{p}{\alpha}, \delta' = \frac{\delta}{\alpha}, m' = \frac{m}{\alpha}, \tau' = \alpha\tau. \quad (\text{A } 4)$$

REFERENCES

- Blasius, B. & Stone, L. 2000 Chaos and phase synchronization in ecological systems. *Int. J. Bifurc. Chaos* **10**, 2361–2380.
- Blasius, B., Huppert, A. & Stone, L. 1999 Complex dynamics and phase synchronization in spatially extended ecological systems. *Nature* **399**, 354–359.
- Costantino, R. F., Desharnais, R. A., Cushing, J. M. & Dennis, B. 1997 Chaotic dynamics in an insect population. *Science* **275**, 389–391.
- Cushing, J. M., Costantino, R. F., Dennis, B., Desharnais, R. A. & Henson, S. M. 2003 *Chaos in ecology: experimental nonlinear dynamics*. Amsterdam: Academic.
- DeAngelis, D. L. 1992 *Dynamics of nutrient cycling and food webs*. London: Chapman & Hall.
- Dennis, B., Desharnais, R. A., Cushing, J. M., Henson, S. M. & Costantino, R. F. 2003 Can noise induce chaos? *Oikos* **102**, 329–339.
- Droop, M. R. 1968 Vitamin B_{12} and marine ecology. IV. The kinetics of uptake, growth and inhibition in *Monochrysis lutheri*. *J. Mar. Biol. Assoc. UK* **48**, 689–733.
- Droop, M. R. 1973 Some thoughts on nutrient limitation in algae. *J. Phycol.* **9**, 264–272.
- Earn, D. J. D., Rohani, P., Bolker, B. M. & Grenfell, B. T. 2000 A simple model for complex dynamical transitions in epidemics. *Science* **287**, 667–670.
- Ebenhöh, W. 1988 Coexistence of an unlimited number of algal species in a model system. *Theor. Popul. Biol.* **34**, 130–144.
- Ebenhöh, W. 1993 Coexistence of similar species in models with periodic environments. *Ecol. Model.* **68**, 227–247.
- Fussmann, G. F., Ellner, S. P., Shertzer, K. W. & Hairston Jr, N. G. 2000 Crossing the Hopf bifurcation in a live predator–prey system. *Science* **290**, 1358–1360.
- Grover, J. P. 1991a Non-steady state dynamics of algal population growth: experiments with two chlorophytes. *J. Phycol.* **27**, 70–79.
- Grover, J. P. 1991b Dynamics of competition among microalgae in variable environments: experimental tests of alternative models. *Oikos* **62**, 231–243.
- Hastings, A. & Powell, T. 1991 Chaos in a three-species food chain. *Ecology* **72**, 896–903.
- Hastings, A., Hom, C. L., Ellner, S., Turchin, P. & Godfray, H. C. J. 1993 Chaos in ecology: is Mother Nature a strange attractor? *A. Rev. Ecol. Syst.* **24**, 1–33.
- Huisman, J. & Weissing, F. J. 1999 Biodiversity of plankton by species oscillations and chaos. *Nature* **402**, 407–410.
- Huppert, A., Blasius, B. & Stone, L. 2002 A model of phytoplankton blooms. *Am. Nat.* **159**, 156–171.
- Hutchinson, G. E. 1961 The paradox of the plankton. *Am. Nat.* **95**, 137–145.
- Kot, M., Saylor, G. S. & Schultz, T. W. 1992 Complex dynamics in a model microbial system. *Bull. Math. Biol.* **54**, 619–648.
- Lange, K. & Oyarzun, F. J. 1992 The attractiveness of the Droop equations. *Math. Biosci.* **111**, 261–278.
- May, R. M. 1974 Biological populations with non-overlapping generations: stable points, stable cycles, and chaos. *Science* **186**, 645–647.
- Monod, J. 1942 *Recherches sur la croissance des cultures bactériennes*. Paris: Hermann.
- O'Brien, W. J. 1974 The dynamics of nutrient limitation of phytoplankton algae: a model reconsidered. *Ecology* **55**, 135–141.
- Pascual, M. 1994 Periodic response to periodic forcing of the Droop equations for phytoplankton growth. *J. Math. Biol.* **32**, 743–759.
- Rinaldi, S. & Muratori, S. 1993 Conditioned chaos in seasonally perturbed predator–prey models. *Ecol. Model.* **69**, 79–97.
- Smith, H. L. 1997 The periodically forced Droop model for phytoplankton growth in a chemostat. *J. Math. Biol.* **35**, 545–556.
- Smith, H. L. & Waltman, P. 1995 *The theory of the chemostat: dynamics of microbial competition*. New York: Cambridge University Press.
- Sommer, U. 1985 Comparison between steady state and non-steady state competition: experiments with natural populations. *Limnol. Oceanogr.* **30**, 335–346.
- Truscott, J. E. 1995 Environmental forcing of simple plankton models. *J. Plankt. Res.* **17**, 2207–2232.
- Vandermeer, J., Stone, L. & Blasius, B. 2001 Categories of chaos and fractal basin boundaries in forced predator–prey models. *Chaos, Solitons Fractals* **12**, 265–276.
- Wolf, A., Swift, J. B., Swinney, H. L. & Vastano, J. A. 1985 Determining Lyapunov exponents from a time series. *Physica D* **16**, 285–317.
- Yoshida, T., Jones, L. E., Ellner, S. P., Fussmann, G. F. & Hairston, N. G. 2003 Rapid evolution drives ecological dynamics in a predator–prey system. *Nature* **424**, 303–306.

As this paper exceeds the maximum length normally permitted, the authors have agreed to contribute to production costs.